Polymer 49 (2008) 2957–2963

Contents lists available at ScienceDirect

Polymer

journal homepage: www.elsevier.com/locate/polymer

Comparison of heat- and pressure-induced gelation of β-lactoglobulin aqueous solutions studied by small-angle neutron and dynamic light scattering

Noboru Osaka [a], Shin-ichi Takata [b], Takuya Suzuki [a], Hitoshi Endo [a], Mitsuhiro Shibayama [a,*]

[a] Neutron Science Laboratory, Institute for Solid State Physics, University of Tokyo, 5-1-5 Kashiwanoha, Kashiwa, Chiba 277-8581, Japan
[b] Japan Atomic Energy Agency, 2-4 Shirane Shirakata, Tokai, Ibaraki 319-1195, Japan

ARTICLE INFO

Article history:
Received 2 March 2008
Received in revised form 22 April 2008
Accepted 27 April 2008
Available online 3 May 2008

Keywords:
β-Lactoglobulin
Gelation
Pressure

ABSTRACT

The gelation mechanism of β-lactoglobulin (bLG) aqueous solutions was investigated by dynamic light scattering (DLS) and small-angle neutron scattering (SANS). Temperature- and pressure-jump experiments, respectively, abbreviated as *T*-jump (from 20 to 75 °C; *T*-jump) and *P*-jump (from 0.1 to 315 MPa) were carried out and the time evolution of gel structure was monitored by DLS and SANS as a function of time. The gelation threshold was determined by DLS as the point when nonergodicity appeared. In the case of *T*-jump, a rapid increase of the time-average scattered intensity, $\langle I \rangle_T$, and a steep decrease of the initial amplitude of the intensity–intensity time correlation function, σ_I^2, were observed at the gelation threshold. On the other hand, *P*-jump showed a gradual increase of the $\langle I \rangle_T$ and a continuous decrease of the σ_I^2. It was revealed by SANS that bLG underwent thermal denaturation, resulting in a formation of gels consisting of densely aggregated unfolded bLG oligomers. On the other hand, the pressure-induced gels were found to be a fractal aggregates consisting of primary particles of bLG monomers. The difference in the gel structure as well as gelation mechanism between bLGs treated by *T*-jump and *P*-jump is discussed in comparison with *T*-induced and *P*-induced microphase separation of amphiphilic block copolymers in water [Osaka N, Shibayama M. Phys Rev Lett 2006;96:048303].

1. Introduction

Denaturation of protein receives much attention from the viewpoints of both fundamental sciences and industrial applications, since it is directly related to the problem of the protein folding [1–3], medicine [4,5], food processing [6] and so on. The denaturation of a globular protein molecule accompanies various kinds of conformational changes, including changes of quaternary, tertiary and secondary structures, which leads to unfolding and aggregation. β-Lactoglobulin (bLG) is known as a major component of bovine milk whey. It is a small protein of *ca.* 18 kDa. Due to its stimuli-sensitive nature, bLG in aqueous solutions has been mainly investigated as a function of temperature, pH, and/or salt concentration [4,7–11]. bLG favors in monomer state at low pH. However, dimer state is more preferable above the isoelectric point (≈pH 5.2) [12]. Upon heating above 50 °C, bLG denatures and aggregates. The structure and mechanism of aggregation depend strongly on pH and ionic strength. For example, at pH 7, the structure of the aggregates is self-similar. On the other hand, loosely tied networks are formed in an acidic condition (e.g., at pH 2) [11,13,14]. These results are supported by the atomic microscopy observation of Ikeda and Morris who reported particulate aggregates in *T*-induced bLG at pH 7 and fine-stranded aggregates at pH 2 [15].

It is well known that pressure is an important variable to determine physical properties of hydrocarbons [16], polymers [17], biomacromolecules [18], and proteins in aqueous solutions [1,19]. bLG molecules unfold above some pressure threshold [20,21]. Panick et al. investigated differences between *P*-induced and *T*-induced denaturation and aggregation of bLG by infrared spectroscopy and small-angle X-ray scattering [21]. Recently, a comprehensive review about functional improvement of bLG by high hydrostatic pressure was given by Lopez-Fandino [12]. The behavior of denaturation and unfolding/refolding of bLG was extensively discussed as a complex function of *P*, *T*, pH, and ionic strength.

Since a *P*-induced protein unfolding accompanies a positive volume change, ΔV, at low pressures and a negative volume change at high pressures (~100–200 MPa), the thermodynamics of *P*-induced denaturation has been a puzzle for more than two decades as "the protein volume paradox" [22]. Recently, Hummer et al. explained this unsolved problem with a concept of water transfer from outside to inside of protein molecules [23]. According to them, a *P*-induced denaturation results in incorporation of water into the interior of the protein, whereas *T*-induced denaturation results in the transfer of nonpolar groups into water. In both cases, the bLG solutions undergo precipitation/gelation depending on the bLG concentration [20].

* Corresponding author.
E-mail address: shibayama@issp.u-tokyo.ac.jp (M. Shibayama).

0032-3861/$ – see front matter © 2008 Elsevier Ltd. All rights reserved.
doi:10.1016/j.polymer.2008.04.055

The denaturation phenomenon can be mimicked by synthetic water-soluble polymers carrying hydrophobic groups. For example, *P*–*T* phase behaviors were investigated for poly(*N*-isopropylacrylamide) (PNIPA) aqueous solutions/hydrogels [17,24–26]. Hydration/dehydration is a common feature of phase change, namely, folding/unfolding and phase-mixing/phase-separation. PNIPA aqueous solutions have a lower-critical solution temperature (LCST) at $T_{LCST} \approx 33\,^{\circ}C$ due to hydrophobic dehydration [27,28]. Because of the simplicity of the chemical structure of PNIPA compared with protein molecules, PNIPA has been used as a model system for studying denaturation of protein. In a previous report, we investigated phase behaviors of poly[2-(2-ethoxy)ethoxyethyl vinyl ether]-*block*-poly(2-methoxyethyl vinyl ether) (pEOEOVE-*b*-pMOVE) aqueous solutions at various temperatures and pressures [29,30]. The pEOEOVE block has an LCST of $T_{LCST} \approx 40\,^{\circ}C$, while pMOVE has an LCST of $T_{LCST} \approx 65\,^{\circ}C$. Hence, pEOEOVE-*b*-pMOVE undergoes a microphase separation in water by heating to a temperature above $T_{LCST} \approx 40\,^{\circ}C$ as confirmed by a series of scattering peaks in small-angle neutron scattering (SANS). However, this *T*-induced microphase separation was strongly suppressed at high pressures (e.g., $P = 300$ MPa). This led to a conclusion that hydrophobic interaction was significantly suppressed by pressurizing. In order to explain this, we proposed a "stone-and-sand mixing model". This explains the negative to positive change of volume in mixing, ΔV, as a function of P [31]. At ambient pressure, ΔV is negative even the volume change of iceberg formation is positive because of the asymmetry of free volumes of the solute and water (solvent). However, the compressibilities of both components become smaller, resulting in a negative to positive change in ΔV. As a result, $dT/dP \equiv T\Delta\overline{V}_m/\Delta H_m$ changes from positive to negative by increasing P, where ΔH_m and $\Delta\overline{V}_m$ are the changes of enthalpy and molar volume by mixing, respectively. The pressure dependence of hydrophobic interaction will be examined in this work based on the results of dynamic light scattering (DLS) and SANS experiments on gelation process of bLG. In this study, we employ a biopolymer, bLG, for studying temperature and pressure dependence of hydrophobic interactions and compare *P*-induced gelation with *T*-induced gelation by using DLS and SANS.

2. Experimental section

2.1. Samples

bLG, crystallized for three times followed by lyophilization, was purchased from Sigma (lot no. 114H7055) which is known to be a mixture of variants A and B. The molecular weight is 1.84×10^4 Da. Aqueous solutions of bLG were prepared by dissolving it in distilled deuterium oxide. The pH of bLG solutions was 7 at ambient pressure. Since it was far from its isoelectric point ($\approx$pH 5.2), we expected that bLG was stable in dimer state. Under high pressure, the equilibrium $CH_3COOH \leftrightarrow CH_3COO^- + H^+$ favors the ionic species. This causes a drop of pH, approximately 0.2–0.3 for every 100 MPa [12,32]. Hence, about 1 unit of pH shift was expected in this study by pressurizing to 300 MPa, which was still above the isoelectric point. The concentration was 0.12 g/ml. Each solution was optically purified with a 0.10 μm filter.

2.2. DLS

DLS experiments were conducted with a static/dynamic compact goniometer (SLS/DLS-5000), ALV, Langen, Germany. A He–Ne laser with a power of 22 mW (wavelength, $\lambda = 6328$ Å) was used as an incident beam. The decay-time distribution functions $G(\Gamma)$ were calculated from the intensity–intensity time correlation function (ITCF), $g^{(2)}(\tau)$, using CONTIN data analysis package [33]. Pressure-dependent DLS experiments were carried out with an inner-cell type pressure cell having a set of optical windows, PCI-400, Teramex, Co. Ltd. Kyoto, Japan [34]. The scattering angle was fixed to be 90°. The temperature of the sample was regulated by circulating water from a NESLAB RTE-111 thermocontroller with the precision of $\pm 0.1\,^{\circ}C$.

2.3. SANS

Pressure-jump SANS experiments were carried out for 0.12 g/ml bLG in deuterated water at SANS-U, the University of Tokyo, installed at JRR-3M reactor guide hall, the Japan Atomic Energy Agency [35]. The wavelength of the neutrons was monochromatized to be 7.0 Å with a mechanical velocity selector. The sample-to-detector distances were 4.0 m, which provided the experimental q-range to be from 0.01 to 0.1 $Å^{-1}$. Pressure-dependent SANS experiments were conducted with a pressure chamber, PCI-400-SANS, Teramex, Co. Ltd. Kyoto, Japan [26]. The applied pressure was transmitted via a rubber diaphragm connected to the inner-cell made of aluminum with quartz and sapphire windows. The sample thickness was 2.0 mm. The outer chamber was filled with D_2O and the pressure was controlled by pressurizing D_2O by a double-cylinder hand pump. The pressure-jump measurements were conducted at $T = 20\,^{\circ}C$. The temperature of the sample was regulated by circulating water with the precision of $\pm 0.1\,^{\circ}C$. Corrections for transmission, air and cell scattering were made before normalizing to the absolute intensity. Temperature-jump SANS measurements were also carried out with the use of the same pressure cell. For the absolute intensity calibration, a polyethylene slab (Lupolen) sample was used [36].

3. Results and discussion

3.1. DLS

Fig. 1(a) shows the normalized ITCF of 0.12 g/ml bLG aqueous solutions obtained by DLS at 20 °C under atmospheric pressure. It is observed that the ITCF starts to decay monotonically at $\tau \approx 0.1$ ms. This figure indicates that the bLG is not aggregated in the aqueous solution at 20 °C under 0.1 MPa. As a matter of fact, bLG is known to be in dimer state at the neutral pH [13,37]. Fig. 1(b) shows the corresponding $G(\Gamma)$, which shows a single peak with the peak position being $\Gamma^{-1} \approx 0.053$ ms. This is assigned to be the translational diffusion of bLG with the hydrodynamic radius, $R_h \approx 40$ Å. This value is in good agreement with the values reported in the previous study (Fig. 2 of Ref. [13]).

In many systems undergoing gelation, such as macromolecules undergoing chemical and/or physical gelation, biopolymers, gelators, etc., the gelation point can be determined by light scattering as (1) an abrupt increase in scattering intensity, (2) a power-law behavior of the intensity–time correlation function (ITCF), (3) a broadening of the distribution function, and (4) suppression of the initial amplitude of ITCF [38,39]. Fig. 2 shows the time evolution of (a) the time-average scattered intensity, $\langle I \rangle_T$, and (b) the initial amplitude of ITCF, σ_I^2, obtained by DLS at 90° during heat-induced (*T*-jump from 20 to 75 °C: open circle) and pressure-induced (*P*-jump from 0.1 to 315 MPa: closed circle) denaturation process. It is observed in Fig. 2(a) that soon after the *T*-jump, the scattered intensity began to increase. On the other hand, the initial amplitude of the ITCF, σ_I^2, remained constant at these regions ($t \approx t_g \leq 0.1$ h), indicating that the solution was in sol state. Here, t_g is the time at which fluctuations in σ_I^2 occurred. Coincidently, the σ_I^2 started to fluctuate and decrease as shown in Fig. 2(b), which meant an ergode–nonergode transition. Therefore, these t_g's are assigned to the gelation thresholds [38]. The gelation threshold will be discussed later in more detail in connection with the change of the

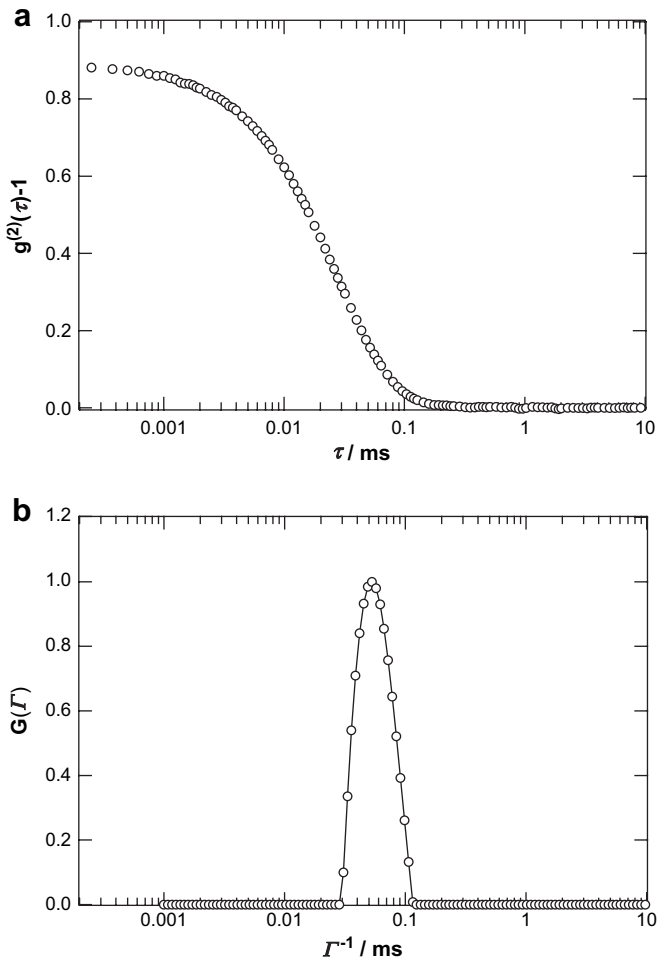

Fig. 1. (a) Correlation function and (b) decay-time distribution function of 0.12 g/ml bLG aqueous solutions obtained by DLS at 20 °C under atmospheric pressure.

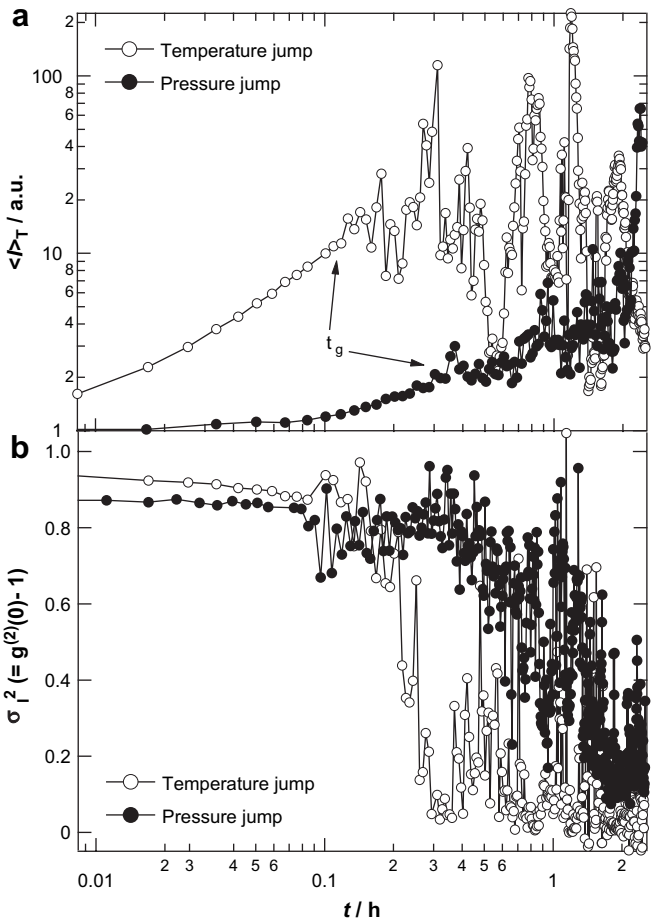

Fig. 2. (a) Time evolution of the scattering intensity, and (b) the initial amplitude of ITCF obtained by DLS at 90° during heat-induced (open circle) and pressure-induced (closed circle) denaturation process. The arrows indicate the onset time of gelation, t_g.

ITCFs. A similar phenomenon was observed for the *P*-jump experiment. However, it should be noted that some distinctions between *T*- and *P*-jump experiments are disclosed. (1) The scattered intensity rise in the *P*-jump experiment is more suppressed than that in the *T*-jump experiment. (2) The t_g in the *P*-jump experiment was much delayed. (3) In contrast with the discrete decrease of σ_I^2 in the *T*-jump experiment, a continuous decrease was observed in the *P*-jump experiment. Though the relative magnitudes of $\langle I\rangle_T$ and σ_I^2 are dependent on the width of the jump, i.e., ΔT and ΔP as well as the initial temperature T_i (or pressure, P_i), the pressure-induced denaturation seems to be more moderate than the heat-induced denaturation. Aymard et al. reported that *T*-induced aggregation of bLG at pH 7 underwent in a two-step process [11]. Such behavior was not observed in the DLS measurement. This might be due to the difference in the residual salt concentrations between the two systems. In the case of bLG at pH 7 with none or very low salt concentrations, *T*-induced aggregation leads to microphase separation [40]. The bLG employed in this work seemed to contain some residues, resulting in no microphase separation by *T*-induced aggregation (e.g., no scattering maximum in SANS as will be shown in Figs. 6 and 8).

Fig. 3 shows the time dependence of ITCFs during *T*-jump (20 → 75 °C) experiments. At the beginning ($t = 0.06$ h), ITCF has a single decay around $\tau \approx 0.1$ ms. After *T*-jump, the decay became slower and slower with time. Near the gelation threshold ($t_g \approx 0.12$ h), the ITCFs showed a power-law behavior. The solid lines are the fits with the following Martin–Wilcoxon–Odinek function [41,42],

$$g^{(2)}(\tau) - 1 = \sigma_I^2 \Big\{ A\exp(-\Gamma_f \tau) + (1-A)\Big[1 + \Big(\tau/\tau^*\Big)\Big]^{(\alpha-1)/2} \Big\}^2 \quad (t \sim t_g) \qquad (1)$$

where Γ and τ^* are characteristic decay rates for the fast mode and the lower cutoff of the slow mode, respectively. A ($0 < A < 1$) is the fraction of the fast mode (collective diffusion). α is the fractal

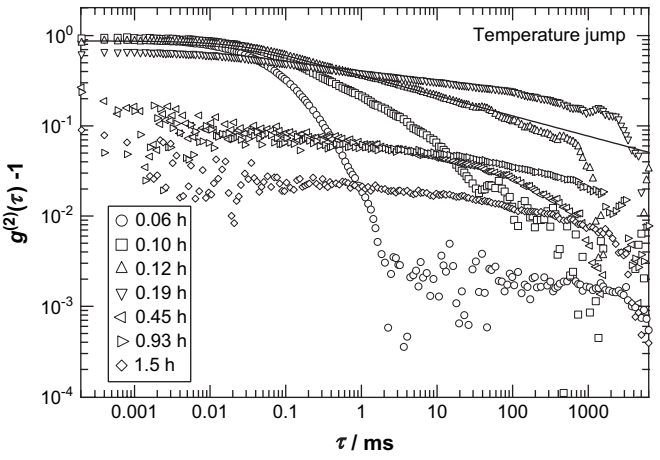

Fig. 3. Time dependence of ITCFs during heat-induced gelation (20–75 °C). The solid curve shows the fit with Eq. (1).

dimension of the scattered photons introduced by Martin et al. for the power-law behavior in DLS. σ_I^2 is the initial amplitude of $g^{(2)}(\tau)-1$, and $\sigma_I^2 \sim 1$ for ergodic systems and $\sigma_I^2 \ll 1$ for non-ergodic systems, respectively. The obtained exponent α was 0.79 ± 0.03 for heat-induced gels by repeating the same experiment for several times with fresh samples. The gelation threshold is consistent with the result in Fig. 2. Such a power-law behavior was often observed in many gelling systems [42–44]. After passing the gelation threshold, the ITCFs became flattened and exhibited $\sigma_I^2 < 1$.

Fig. 4 shows the time dependence of ITCFs during *P*-jump (0.1 to 315 MPa) experiments. Soon after the *P*-jump ($t = 0.06$ h), ITCF has a single decay around $t \approx 0.1$ ms. A similar time evolution of ITCFs to those obtained by the *T*-jump experiment was observed. Near the gelation threshold ($t_g = 0.37$ h), the ITCF showed a power-law behavior, which is well fitted with Eq. (1) (the solid line). The obtained exponent α was 0.83 ± 0.03 irrespective of repetition of the same experiments for several times with fresh samples. From this result, it is confirmed that the bLG solutions also undergo denaturation by *P*-jump. The difference of the mechanisms between *P*-induced and *T*-induced gelation will be discussed later.

3.2. SANS

In comparison with DLS, SANS seems to be less sensitive to the gelation threshold if a polymer solution becomes a gel by introduction of cross-links. This is because the spatial window of SANS, i.e., a few tens to hundreds angstroms, is much smaller than the one characteristic of gel structure. In addition, cross-linking often does not lead to significant change in the concentration fluctuations because it is not a transition of concentration fluctuation, but a transition of connectivity [45]. However, a gelation process can be monitored by SANS as a gradual change if polymerization and/or aggregation of small-size molecules are involved. Gelation and aggregation are one of such cases since bLG molecules can be regarded as "small" molecules and polymerization and/or aggregation are expected to occur by *T*- or *P*-jump. First of all, let us show the time evolution of the SANS scattering intensity, $I(q)$, at a fixed $q = 0.0115$ Å^{-1} as a function of time in Fig. 5. Similar to the case of the time-resolved DLS experiments (Fig. 2), the SANS intensity increases both by *T*- and *P*-jump. The scattering intensity rise of *T*-jump is much faster and larger than that of *P*-jump. This indicates that *T*-induced protein denaturation is more drastic than *P*-induced denaturation.

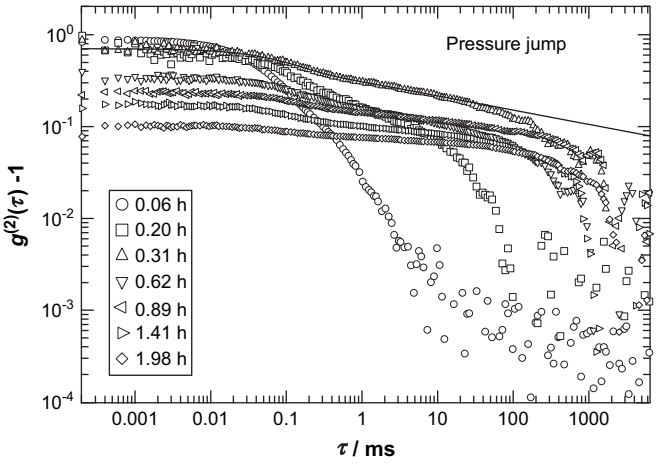

Fig. 4. Time dependence of ITCFs during pressure-induced gelation (0.1–315 MPa). The solid curve shows the fit with Eq. (1).

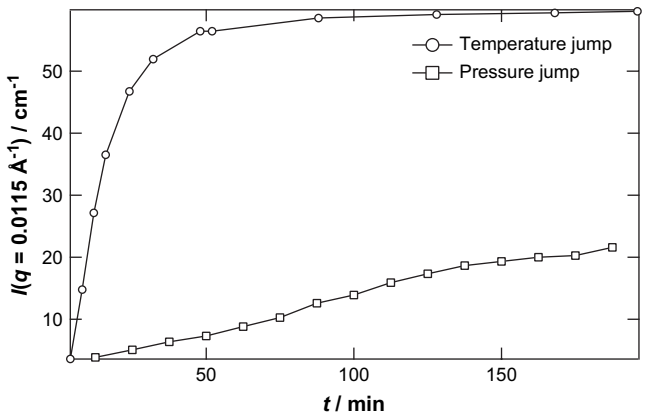

Fig. 5. Time evolution of the SANS intensity, $I(q)$, at $q = 0.0115$ Å^{-1} for *T*-jump and *P*-jump.

Fig. 6 shows a series of the SANS intensity curves, $I(q)$s, during *T*-induced gelation under atmospheric pressure. At 20 °C, before starting the *T*-jump, $I(q)$ (open circles) has a very shallow peak around $q = 0.05$ Å^{-1}, indicating the presence of the inter-particle interference with the distance of 125 Å. This SANS profile is successfully fitted with a Percus–Yevick equation with the core radius of 23.7 Å and the inter-particle distance of 105 Å. Hence, globular proteins of radius of R_g are packed rather irregularly with a hard core potential. Soon after the *T*-jump, the SANS intensity began to increase at low q region, i.e., $q \geq R_{g^{-1}}$, the radius of gyration of the globular protein. This means that an increase of the concentration fluctuations occurs in the spatial range greater than the size of the globular protein. Coincidentally, the decrease of the SANS intensity at high q region was observed, which indicated the sharpening of the surface of the particle unit. It should be noted here that no drastic change was observed in the SANS curve in the vicinity of the gelation threshold ($t_g \sim 6$ min) in comparison with the DLS results. After 48 min, no further change was detected at these q ranges (Fig. 6).

We analyzed the SANS intensity curves during *T*-jump by fitting. In general, the SANS intensity curve, $I(q)$, is given by $I(q) = F(q)S(q)$, where $F(q)$ is the form factor representing the shape of the particle and $S(q)$ is the structure factor representing the inter-particle

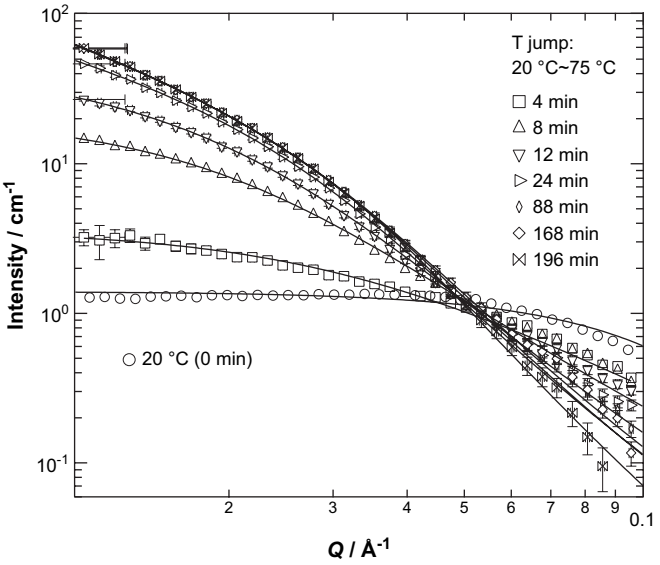

Fig. 6. Time evolution of the scattering curve obtained by SANS during heat-induced gelation at 0.1 MPa. The solid curves are the fitting curves with Eqs. (2) and (3).

interaction. Here, we used the hard sphere as the $F(q)$, which is given by

$$F(q) = \left\{\frac{3[\sin(qR) - qR\cos(qR)]}{(qR)^3}\right\}, \quad (2)$$

where R is the radius of the globular protein. The polydispersity of the sphere size was convoluted in the $F(q)$ as a Gaussian distribution function. Also, we used the Freltoft–Kjems–Sinha function for fractal aggregates as the $S(q)$ [46], which is given by

$$S(q) = 1 + \frac{C\left(d_f - 1\right)\Gamma\left(d_f - 1\right)\xi^{d_f}}{\left(1 + q^2\xi^2\right)^{d_f/2}} \frac{\left(1 + q^2\xi^2\right)^{1/2}}{q\xi} \times \frac{\sin\left[\left(d_f - 1\right)\arctan(q\xi)\right]}{d_f - 1} \quad (3)$$

where C is a constant and d_f is the fractal dimension of the aggregate and $\Gamma(x)$ is the gamma function of argument x, and ξ is the correlation length of the aggregate [46]. The scattering curves are well reproduced by the solid lines as shown in Fig. 6. At 196 min, R was 73 Å and d_f was 1.40 from the fitting result. The size of R is much larger than the hydrodynamic radius ($R_h = 40$ Å) and the core radius at 20 °C ($R \approx 23.7$ Å). Therefore, it is considered that the particle unit of the gels is an aggregate of a few bLG molecules, i.e., oligomers. This strongly agglutinative aggregation is derived by the hydrophobic interaction of the protein at ambient pressure [21]. $d_f = 1.40$ is smaller than one generally obtained in three dimension ($2.0 < d_f < 3.0$). However, this result is often observed in any other system [47]. In addition, ionic strength dependence of the d_f, where the value can be smaller than 2.0, was observed in the previous study of the bLG [48]. Fig. 7 shows the time evolution of the unit size of aggregates R and the fractal dimension, d_f. As sooner as T-jump, both R and d_f increase very steeply within 12 min (the third point), followed by saturation. Hence, it is concluded that the heat-induced denaturation is a very rapid process with strongly agglutinative aggregation.

Next, let us discuss the result of pressure-dependent SANS experiment. Up to 140 MPa, no distinct change of the scattering curves was observed as shown in Fig. 8 and leaving the solution for 1 h at 140 MPa resulted in no time evolution of the scattering curve. The stability of bLG against hydrostatic pressure in a low pressure region was also reported by Belloque et al. by NMR [12,49,50]. Therefore, we carried out P-jump experiment from 140 to 315 MPa at 20 °C. Soon after the onset of the P-jump experiment, the SANS intensity increased as shown in Fig. 9. Note that $I(q)$s are power-low functions of q. The SANS curves could be fitted by Eqs. (2) and (3). Neither significant change of the SANS curve nor a power law behavior was observed after 187.5 min.

Fig. 10 shows the variation of the fitted parameters, i.e., R and d_f. In comparison with the result of the T-jump experiment, R is significantly smaller, indicating that the degree of unfolding of bLG is much less than that of T-jump. The value of d_f, on the other hand, is larger and increases with P. Note that clear power-law behaviors are seen in P-denatured gels. This indicates that P-denatured gels are formed by fractal aggregates having a large distribution with fine-stranded clusters ($R \approx 40$ Å).

3.3. Comparison of heat-induced and pressure-induced denaturation

Here, we discuss the structures of bLG after T-induced and the P-induced denaturations. In the case of the former, strong hydrophobic interaction dominates aggregation process. Hence, a few bLG molecules aggregate to each other to oligomers. Gelation takes

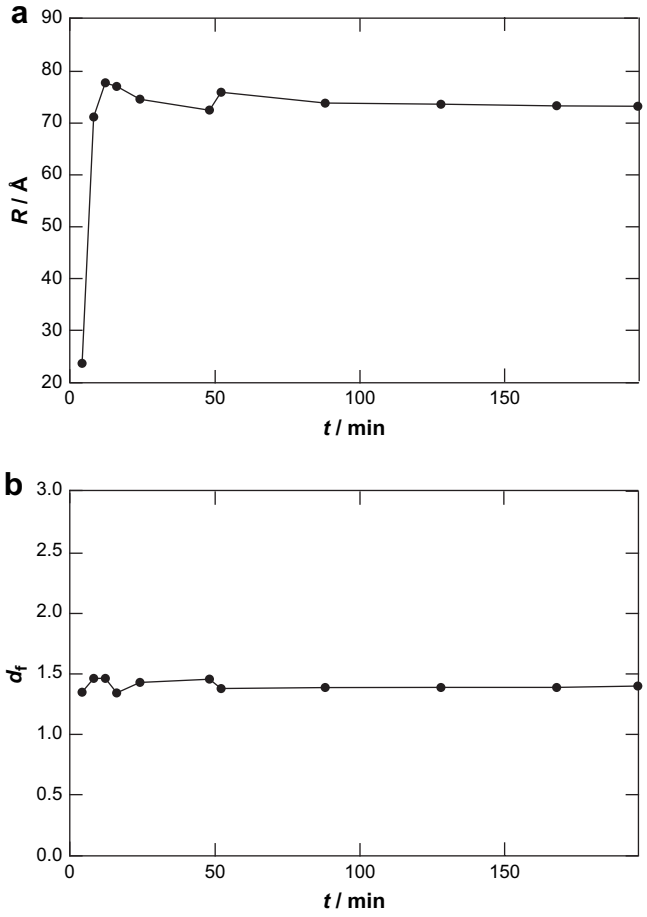

Fig. 7. Time dependence of (a) the radius of the aggregation units and (b) the fractal exponents of the aggregates obtained by using Eqs. (2) and (3) during heat-jump.

place by clustering these units (Fig. 11 left). On the other hand, in the case of P-induced denaturation, partial unfolding of bLG leads to chains consisting of primary particles, having a broad distribution of the cluster size and occasional branching (Fig. 11 right). Ikeda and Morris carried out morphological studies of bLG aggregates by atomic force microscopy [15]. According to their work, fine-

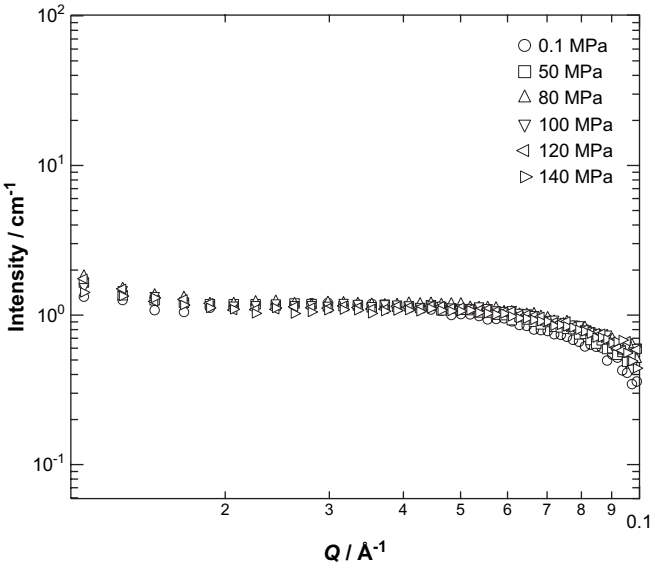

Fig. 8. SANS intensity curves at low pressures (0.1–140 MPa).

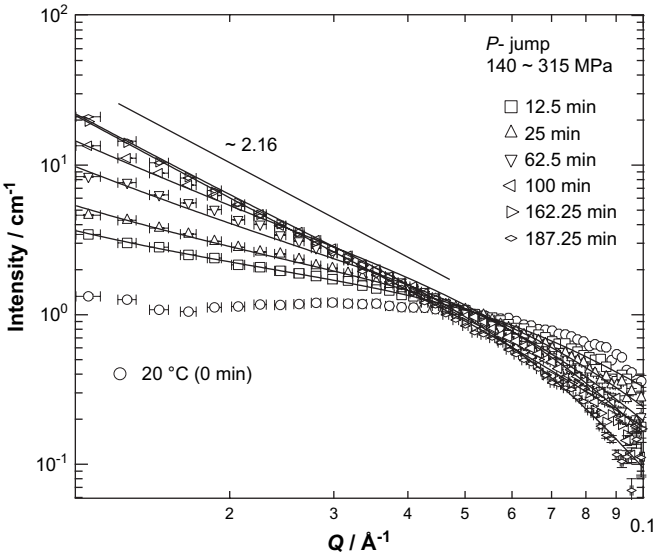

Fig. 9. Time evolution of the scattering curve obtained by SANS during pressure-induced gelation at 20 °C. The solid line indicates a line of a power-law with 2.16.

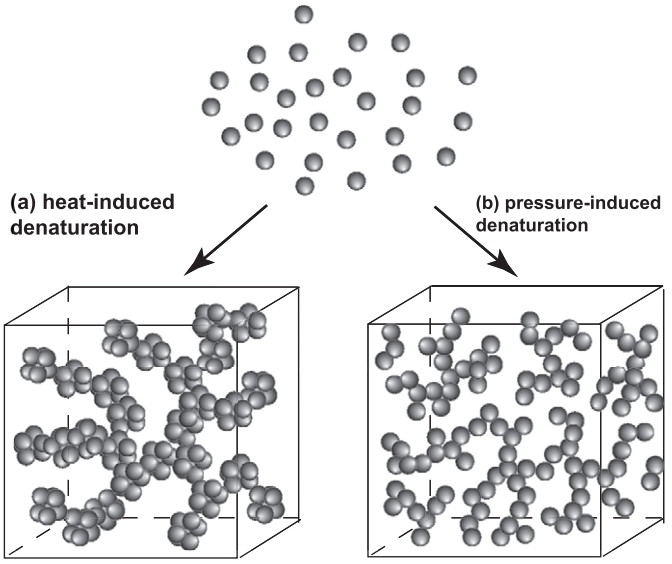

Fig. 11. Schematic illustration of gelation of bLG by heat-induced (left) and pressure-induced denaturation (right). The heat-induced denatured gels are formed by densely aggregated proteins globules, while the pressure-induced denatured gels are fractal aggregates with primary particles of bLG.

stranded aggregates consisting of individual primary particles, i.e., bLG monomer, and particulate aggregates made of aggregated primary particles are formed at pHs 2 and 7, respectively. Our observation of bLG gels formed by *P*-induced gelation seems to be closer to the one made by heat denaturation at pH 2, but is different from either gels made at pHs 2 and 7 because it has a higher fractal dimension than that expected for fine-stranded chains. It should be noted that rheological measurements were carried for *T*-denatured and *P*-denatured proteins [51]. They reported that *P*-denatured gel is more porous than *T*-denatured one, which is contradictory to our results. However, their measurement was done after cooling or after releasing *P*. In their case, voids might have been expanded by depressurizing. Our experiments, on the other hand, were carried out "in situ". To our knowledge, there are no papers dealing with "in situ" rheological properties of *P*-denatured gels. Hence, the *P*-denatured gels seem to be classified into another class of gels which consist of fine-strands but have a higher degree of branching than those by *T*-denatured gels at pH 2.

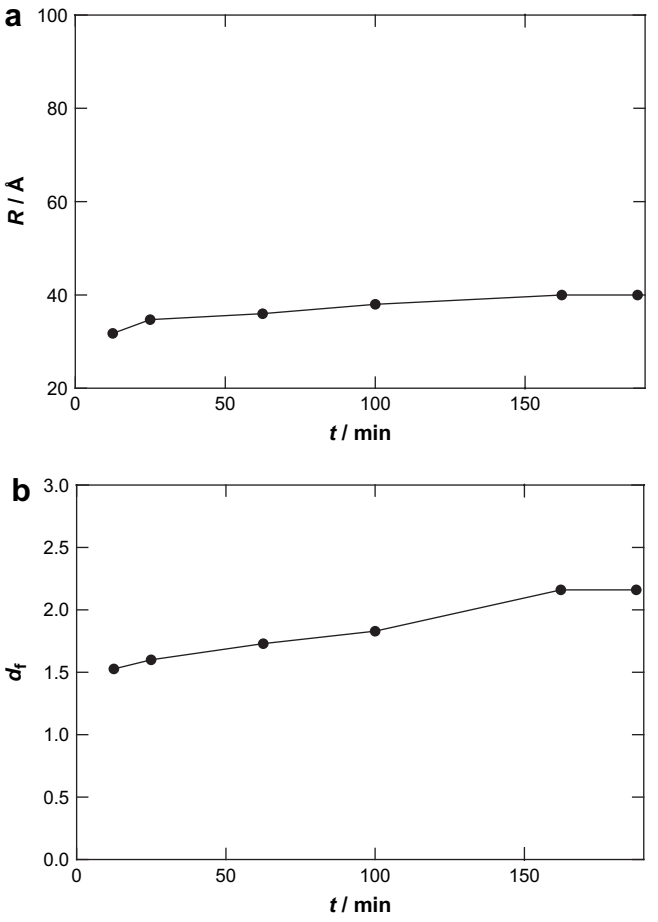

Fig. 10. Time dependence of (a) the radius of gyration of the cross-linking chain and (b) the fractal exponents of the aggregates obtained using Eqs. (2) and (3) during pressure-jump.

The difference in the gelation process may lie in the role of heating vs pressurizing. Heating can change the molecular structure of bLG by dissociating hydrogen bonds, hydrophobic bonds, and disulphide bonds, while pressurizing simply compresses bLG molecules, which may destroy hydrophobic hydration. Pressurizing may also work to fill the cavity in bLG molecules by filling water. As Hummer et al. discussed, pressure-denatured bLG, unlike heat-denatured bLG, retain a compact structure with water penetrating their core [23]. As a result, heating is more harsh than pressurizing. *T*-induced denaturation may lead to unfolding of bLG, followed by formation of larger globules by assembling a few numbers of bLG molecules. This results in formation of dendric clusters. On the other hand, *P*-induced denaturation promotes partial unfolding and only a few functional groups are activated which play as a bonding to neighboring bLG. As a result, fine-stranded clusters are formed. This conjecture is consistent with the model discussed by Lopez-Fandino [12]. It is reported that tryptophan residues in bLG in an aqueous solutions become part of a more hydrophilic by pressurizing [52] and the positive virial coefficient of the bLG decreases [53]. These results mean that the affinity of the protein to water increases by pressurizing. This phenomenon is regarded as a weakening of hydrophobic interaction between protein and water. Due to the weakening of the hydrophobic interaction, the particle unit of the fractal aggregates obtained by pressurizing is smaller than one obtained by heating at ambient pressure. This difference of the aggregation behavior is observed in the previous studies using block copolymer aqueous solutions. A robust

microphase separated structure was formed at ambient pressure due to the distinct hydrophobic interaction [29,30]. On the other hand, distorted microphase separation was observed at high pressure due to the weakening of the hydrophobic interaction. Hence, a similar effect in hydrophobic interaction was observed by pressurizing in both the proteins and the synthetic polymers.

4. Conclusion

Time-resolved DLS and SANS investigation was carried out for gelation process of bLG aqueous solutions after *T*- (from 20 to 75 °C) and *P*-jump (from 0.1 to 315 MPa). The gelation thresholds were determined using DLS. SANS results clearly show the difference in the *T*-induced and *P*-induced denaturation. In the case of *T*-jump, fractal aggregates consisting of a coarsely branched network (a fractal dimension $d_f \approx 1.4$) with densely aggregated proteins globules are formed. On the other hand, *P*-jump results in a moderate denaturation compared with *T*-jump and individual protein globules are less unfolded to form fine-stranded self-similar clusters with $d_f \approx 2.2$. This type of *P*-induced denaturation is ascribed to lowering of the hydrophobic interaction at high pressure, followed by gradual denaturation. This finding, i.e., the weakening of hydrophobic interaction with pressurizing, in another word, a weakening of hydrophobic bonding by pressurizing, is consistent with our previous studies by using water-soluble synthetic polymers as a model for understanding proteins.

Acknowledgement

This work was also partially supported by the Ministry of Education, Science, Sports and Culture, Japan (Grant-in-Aid for Scientific Research (A), 2006–2008, No. 18205025, and for Scientific Research on Priority Areas, 2006–2010, No. 18068004). The SANS experiment was performed with the approval of Institute for Solid State Physics, The University of Tokyo (Proposal Nos. 06.237), at Japan Atomic Energy Agency, Tokai, Japan.

References

[1] Kauzmann W. Nature 1987;325:763–4.
[2] Creighton TE. Biochem J 1990;270:1–16.
[3] Deniz AA, Laurence TA, Beligere GS, Dahan M, Martin AB, Chemla DS, et al. Proc Natl Acad Sci 2000;97:5179.
[4] Papiz MZ, Sawyer L, Eliopoulos EE, North ACT, Findlay JBC, Sivaprasadarao R, et al. Nature 1986;324:383–5.
[5] Bukau B, Horwich A. Cell 1998;92:351–66.
[6] Trujillo AJ, Capellas M, Saldo J, Gervilla R, Guamis B. Innovat Food Sci Emerg Technol 2002;3:295–307.
[7] Kelly MJ, Reithel FJ. Biochemistry 1971;10:2639–44.
[8] Pessen H, Purcell JM, Farrell Jr HM. Biochim Biophys Acta 1985;928:1–12.
[9] Griko YV, Privalov PL. Biochemistry 1992;31:8810–5.
[10] Gimel JC, Durand D, Nicolai T. Macromolecules 1994;25:583–9.
[11] Aymard P, Gimel JC, Nicolai T, Durand D. J Chim Phys 1996;93:987–97.
[12] Lopez-Fandino R. Crit Rev Food Sci Nutr 2006;46:351–63.
[13] Takata S, Norisuye T, Tanaka N, Shibayama M. Macromolecules 2000;33:5470–5.
[14] Arnaudov LN, Stuart MAC. J Chem Phys 2006;124:084701.
[15] Ikeda S, Morris VJ. Biomacromolecules 2002;3:382–9.
[16] Sawamura S, Kitamura K, Taniguchi Y. J Phys Chem 1989;93:4931–5.
[17] Kunugi S, Takano K, Tanaka N. Macromolecules 1997;30:4499–501.
[18] Smeller L. Biochim Biophys Acta 2002;1595:11–29.
[19] Heremans K, Smeller L. Biochim Biophys Acta 1998;18:353–70.
[20] Dumay EM, Kalichevsky MT, Cheftel JC. J Agric Food Chem 1994;42:1861–8.
[21] Panick G, Malessa R, Winter R. Biochemistry 1999;38:6512–9.
[22] Chalikian TV, Breslauer KJ. Biopolymers 1996;39:619–26.
[23] Hummer G, Garde S, Garcia AE, Paulaitis ME, Pratt LR. Proc Natl Acad Sci 1998;95:1552–5.
[24] Kato EJ. Chem Phys 1997;106:3792–7.
[25] Kunugi S, Tanaka N. Biochim Biophys Acta 2002;1595:329–44.
[26] Shibayama M, Isono K, Okabe S, Karino T, Nagao M. Macromolecules 2004;37(8):2909–18.
[27] Hirokawa Y, Tanaka T. J Chem Phys 1984;81:6379–80.
[28] Schild HG. Prog Polym Sci 1992;17:163–249.
[29] Osaka N, Shibayama M. Phys Rev Lett 2006;96(4):048303.
[30] Osaka N, Okabe S, Karino T, Hirabaru Y, Aoshima S, Shibayama M. Macromolecules 2006;39:5875–84.
[31] Nasimova IR, Karino T, Okabe S, Nagao M, Shibayama M. Macrmolecules 2004;37(23):8721–9.
[32] Kitamura Y, Itoh T. J Solution Chem 1987;16:715–25.
[33] Provencher SW. Comput Phys Commun 1982;27:213–27.
[34] Matsumoto M, Murakoshi K, Wada Y, Yanagida S. Chem Lett 2000;29(8):938–9.
[35] Okabe S, Nagao M, Karino T, Watanabe S, Adachi T, Shimizu H, et al. J Appl Crystallogr 2005;38:1035–7.
[36] Shibayama M, Nagao M, Okabe S, Karino T. J Phys Soc Jpn 2005;74:2728–36.
[37] Aymard P, Durand D, Nicolai T. Int J Biol Macromol 1996;19:213.
[38] Shibayama M, Norisuye T. Bull Chem Soc Jpn 2002;75:641–59.
[39] Shibayama M. Bull Chem Soc Jpn 2006;79:1799–819.
[40] Nicolai T, Pouzot M, Durand D, Weijers M, Visschers RW. Europhys Lett 2006;73:299–305.
[41] Martin JE, Wilcoxon J, Odinek J. Phys Rev A 1991;43:858–71.
[42] Martin JE, Wilcoxon J. Phys Rev Lett 1988;61:373–5.
[43] Adam M, Delsanti M, Munch JP, Durand D. Phys Rev Lett 1988;61:706–9.
[44] Norisuye T, Shibayama M, Tamaki R, Chujo Y. Macromolecules 1999;32:1528–33.
[45] Norisuye T, Shibayama M, Nomura S. Polymer 1998;39(13):2769–75.
[46] Freltoft T, Kjems JK, Sinha SK. Phys Rev B 1986;33:269–75.
[47] Weitz DA, Oliveria M. Phys Rev Lett 1984;52:1433–6.
[48] Pouzot M, Nicolai T. Macromolecules 2004;37.
[49] Belloque J, Smith GM. J Agric Food Chem 2000;48.
[50] Belloque J, Chicon R, Lopez-Fandino R. J Agric Food Chem 2007;55:5282–8.
[51] Van Camp J, Huyghebaert A. Food Chem 1995;54:357–64.
[52] Valente-Mesquita VL, Botelho MM, Ferreira ST. Biophys J 1998;75:471–6.
[53] Loupiac C, Bonetti M, Pin S, Calmettes P. Biochim Biophys Acta 2006;1764.